Tuning polymers grafted on upconversion nanoparticles for the delivery of 5-fluorouracil

Alireza Kavand, Nicolas Anton, Thierry Vandamme, Christophe Serra, Delphine Chan-Seng

Tuning polymers grafted on upconversion nanoparticles for the delivery of 5-fluorouracil

Alireza Kavand,[a,b] Nicolas Anton,[b] Thierry Vandamme,[b] Christophe A. Serra,[a] Delphine Chan-Seng[a,]*

[a]Université de Strasbourg, CNRS, Institut Charles Sadron UPR 22, F-67000 Strasbourg, France

[b]Université de Strasbourg, CNRS, Laboratoire de conception et application de molécules bioactives UMR 7199, F-67000 Strasbourg, France

* corresponding author: delphine.chan-seng@ics-cnrs.unistra.fr (D. Chan-Seng)

ABSTRACT

Efficient and safe delivery of anticancer drugs such as 5-fluorouracil (5-FU) is still a challenge in chemotherapy. The combination of polymers with a luminescent probe offers a promising venue to develop nanoobjects for theranostics. Herein, upconversion nanoparticles (UCNPs) decorated with polymers based on *N*-(2-hydroxypropyl) methacrylamide at their surface were investigated as potential carriers of 5-FU. The hyperbranched topology of the polymer offered a higher loading capacity of the polymer shell as compared to this linear analog even though the loading in 5-FU remained low and its release was fast (few hours). To overcome these limitations, 5-FU was conjugated to the polymer through esterification leading to a four-fold increase of the loading and a more sustained release over few days. The introduction of branching points with a disulfide bridge on the polymer afforded nanohybrids susceptible to degradation in the reductive environment of cancer cells. The degradation of the polymer was confirmed by incubating the polymer with dithiothreitol. These results pave the way to theranostics through the use of luminescent properties of UCNPs and the tuning of the polymer architecture.

KEYWORDS: Hyperbranched polymer, upconversion nanoparticle, drug delivery, 5-fluorouracil, redox-degradable branching points

1. INTRODUCTION

Theranostics is a fascinating field in biomedicine combining the delivery of a therapeutic drug and diagnostics through bioimaging on a same carrier.[1] While bioimaging is strongly dominated by the use of organic dyes,[2] the development in nanotechnologies has influenced this field leading notably to the use of inorganic nanoparticles.[3] A wide range of nanoparticles have been investigated including iron oxide nanoparticles for magnetic resonance imaging,[4, 5] but also quantum dots[6, 7] and upconversion nanoparticles[8-10] (UCNPs) as optical contrast agents. Lanthanide-doped UCNPs are anti-Stokes shift luminescent materials able to convert low energy excitation (*i.e.* near-infrared (NIR) excitation) into higher energy emission (*i.e.* visible and ultraviolet (UV-vis) emission). These materials have recently received an increased interest as bioimaging probes due to their properties including high optical penetration depth of light in biological tissues, low phototoxicity, and high signal-to-noise ratio. However, UCNPs generally are capped with hydrophobic ligands altering their dispersion in aqueous solution and suffer from limited stability in aqueous media, which has led to the development of various strategies to modify their surface including adding polymers at the surface of UCNPs. Polymers can be introduced either by ligand exchange using polymers bearing anchoring moieties (*e.g.* amine,[11] carboxylic acid,[11-13] sulfonic acid,[12, 14] phosphate,[12, 15] and phosphonates[16]), or by performing polymerization at or from the surface of UCNPs. Wu *et al.* have removed the oleic acid ligands from the surface of UCNPs by acid treatment to induce the electrostatic adsorption of dopamine that was polymerized under oxidative conditions.[17] UCNPs have also been explored to trigger photopolymerization upon NIR irradiation in the presence of Eosin Y as photoinitiator to prepare crosslinked polymers at the surface of UCNPs.[18, 19] Ricinoleic acid has been used as ligand to prepare UCNPs bearing hydroxyl groups able to initiate cationic ring-opening polymerization from the surface of UCNPs for the synthesis of hyperbranched polyglycerol[20, 21] and linear poly(ε-caprolactone)[21] affording UCNPs with high water dispersibility and upconversion luminescence. Polymerization at the surface of UCNPs has been also considered by building up a silica shell with suitable functional groups around the UCNPs. UCNPs with a silica shell bearing thiol groups have permitted the introduction of oxime-ester coumarin photoinitiators able to initiate thiol-ene and conventional radical polymerization from their surface,[22] while the presence of amines on the silica shell have permitted the insertion of the suitable initiators for atom transfer radical polymerization[23] or chain transfer agents for reversible addition-fragmentation chain transfer (RAFT) polymerization[24, 25] used to grow methacrylate-based polymer from the surface of UCNPs.

We recently reported the polymerization of *N*-(2-hydroxypropyl) methacrylamide (HPMA) with linear and hyperbranched topologies from the surface of UCNPs (UCNP@polyHPMA and UCNP@HBP respectively)

under RAFT conditions.[26] UCNP@HBP showed a strong emission exhibiting their potential as imaging probes. If the polymer shell could be tuned to induce controlled release of a drug, these nanoobjects could be promising for theranostics. 5-Fluorouracil (5-FU) was chosen as model drug for this work. 5-FU is an anticancer agent used for the treatment of a wide range of cancers,[27, 28] but its short plasma half-life, low selectivity towards cancer cells, and severe side effects have limited its clinical use.[29, 30] Recent developments have aimed at improving its bioavailability through encapsulation in polymer particles[31-33] or liposomes,[34] but also the preparation of prodrugs[35] and its conjugation to polymers.[36-38] Herein, UCNPs decorated with linear and hyperbranched poly(*N*-(2-hydroxypropyl) methacrylamide) were investigated as 5-FU carriers though passive encapsulation in the polymer shell or conjugation to the polymer. The structure of the polymers was further tuned through the insertion of redox-degradable branching points to trigger the release of 5-FU under conditions specifically met in cancer cells.

2. RESULTS AND DISCUSSION

2.1. Passive loading of 5-FU in UCNP@polyHPMA and UCNP@HBP

The RAFT polymerization of HPMA was performed from UCNP functionalized with 0.24 mmol of 4-cyano-4-(thiobenzoylthio)pentanoic acid (CPABD) per gram of UCNPs (UCNP@CPABD) having a diameter of 45 nm as previously described.[26] Nanohybrids with linear (UCNP@polyHPMA) and hyperbranched polymers (UCNP@HBP with a degree of branching of 0.17) were prepared. The synthesis of UCNP@HBP was conducted in the presence of 4-cyano-4-(phenylcarbonothioylthio)pentanoate (MA-CPABD) as transmer inducing the formation of branching points. These nanohybrids had roughly the same amount of polymer grafted at their surface (44 and 42 wt% respectively), while their respective molecular weights were 1,794,000 g mol^{-1} (Đ = 3.15) and 220,000 g mol^{-1} (Đ = 6.75).

The nanohybrids dispersed in water (3.3 mg mL^{-1}) were passively loaded by incubating them at room temperature for 24 h varying the amount of 5-FU used from 0.7 to 3.3 mg mL^{-1} (*i.e.* feed in drug of 16 to 50 wt% relative to the nanohybrids). The drug loading (**Fig. 1**) was determined by UV spectroscopy using a calibration curve of 5-FU in water established with the characteristic absorbance of 5-FU at 265 nm (**Fig. S1**). The drug loading increased from 0.5 to 1.5 wt% for UCNP@polyHPMA and from 0.7 to 3.1 wt% for UCNP@HBP when increasing the feed in drug from 16 to 50 wt%. These results indicated a higher encapsulation efficiency of HBPs to load 5-FU as compared to polyHPMA (**Fig. S2**) attributed to the formation of internal cavities in the HBP structure promoting a better retention of the drug.[39, 40] However, the low drug loading for these systems could be detrimental for a use as drug delivery system.

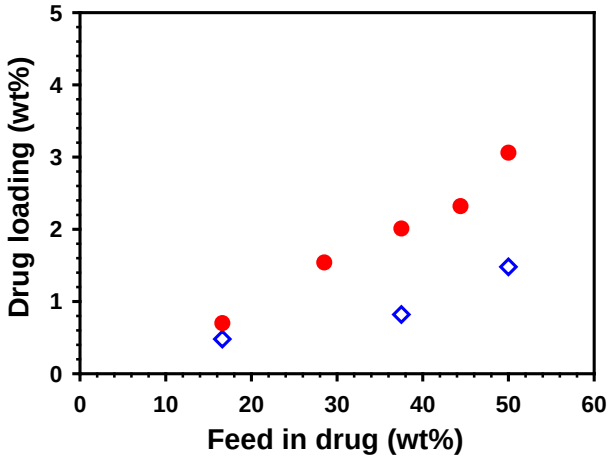

Fig. 1. Evolution of the passive loading of 5-FU as a function of the concentration in drug in the feed for UCNP@polyHPMA (open blue diamonds) and UCNP@HBP (filled red circles) at a concentration of 3.3 mg mL^{-1} in water after 24 h of incubation at room temperature.

The cumulative amount of drug released (**Fig. 2**) was monitored for 5-FU-loaded UCNP@HBP by placing it in a phosphate buffer solution (PBS) at pH 7.4 and 37 °C withdrawing aliquots in triplicate at predetermined times. The results indicated that at least 70 % of 5-FU loaded in UCNP@HBP was released with the first 4 h reaching a plateau. This burst release was attributed to the hydrophilicity of 5-FU and the polymer, which did not act as a barrier against the diffusion of this drug of small size. This nanocarrier was thus not suitable to be used for drug delivery as 5-FU would be released while the carrier would be circulating in the blood stream before reaching the targeted site.

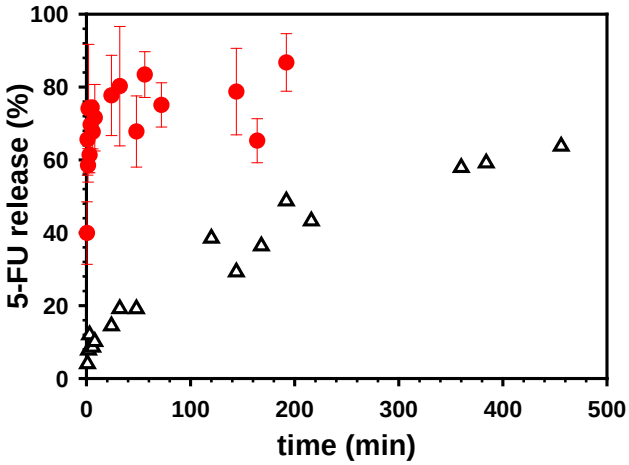

Fig. 2. Drug release profile of 5-FU passively loaded (filled red circles, experiments conducted in triplicate) or conjugated (open black triangles) on UCNP@HBP in PBS at 37 °C and pH 7.4.

2.2. Conjugation of 5-FU on UCNP@HBP through ester linkages

To improve the encapsulation stability in the blood stream and increase the drug loading, drug conjugation was considered, in which the drug is covalently bound to the nanocarrier and its release occurs thanks to a labile bond. Due to the number of hydroxyl groups on polyHPMA,[41] the drug conjugation was considered through reaction of these groups with a carboxylic acid present on the drug to promote the formation of an ester linkage that is hydrolytically degradable in physiological conditions in the presence of esterase or hydrolytic enzymes, but also catalyzed with acids or bases.[42] As 5-FU does not have a carboxylic group, 5-fluorouracil-1-acetic acid (5-FU-COOH) was prepared as previously reported by Sun *et al*., which reported a relatively lower potency of 5-FU-COOH as compared to 5-FU as anticancer drug in HeLa and SGC-7901 cells.[38] 5-FU-COOH was then conjugated to the polymer backbone of UCNP@HBP by esterification reaction (**Scheme 1**) using *N*,*N*,*N*′,*N*′-tetramethyl-O-(1H-benzotriazol-1-yl)uronium hexafluorophosphate (HBTU) as coupling agent in the presence of *N*,*N*-diisopropylethylamine (DIPEA) in DMF. After purification by performing cycles of centrifugation followed by redispersion in water, the presence of 5-FU covalently attached on the nanohybrids was confirmed by FT-IR spectroscopy by the presence of additional peaks at 1243 and 1699 cm^{-1} when compared to UCNP@HBP (**Fig. 3**) attributed to the C-F stretching bands and the C=O group of pyrimidine ring of 5-FU respectively.

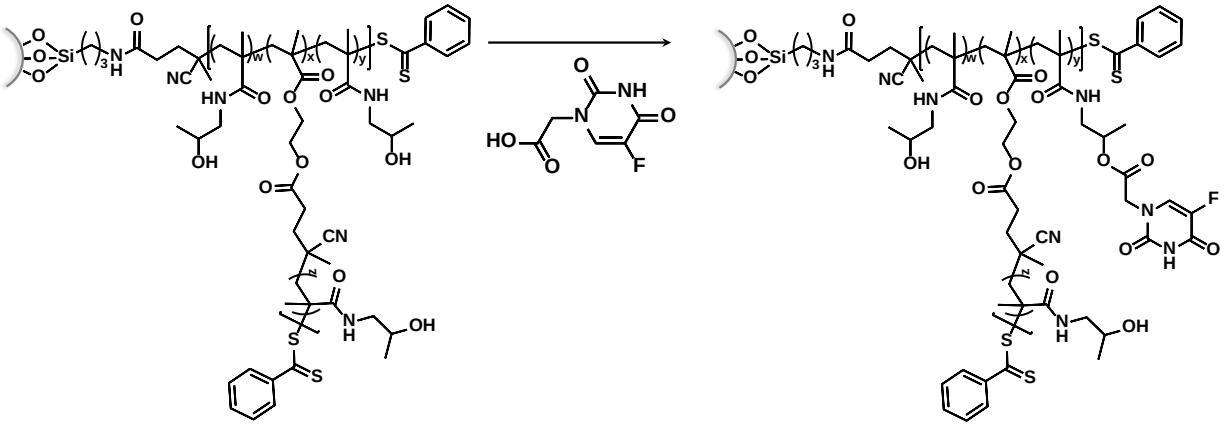

Scheme 1. Conjugation of 5-FU-COOH on UCNP@HBP.

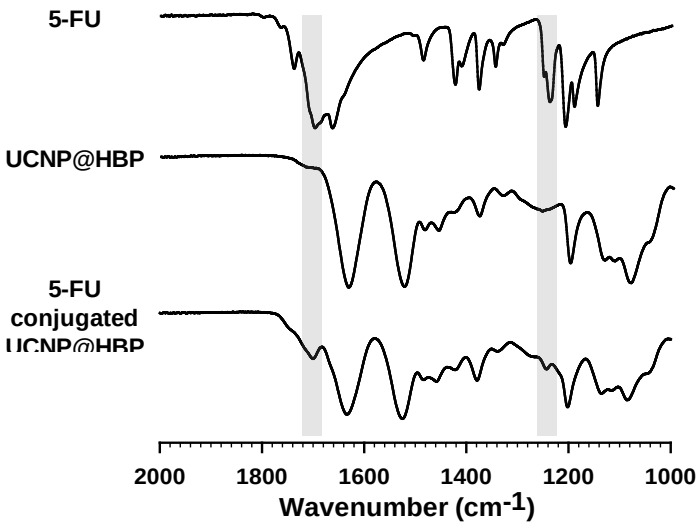

Fig. 3. FTIR spectra of 5-FU, UCNP@HBP, and 5-FU-conjugated UCNP@HBP (the characteristic peaks of the conjugation of 5-FU on UCNP@HBP are highlighted in grey).

The loading in 5-FU for 5-FU-conjugated UCNP@HBP was determined by hydrolyzing all the ester bonds linking the drug to the polymer under basic conditions and recovering 5-FU from the supernatant after centrifugation. The amount of 5-FU was determined as 12 wt% by UV spectroscopy measuring the characteristic absorbance of 5-FU at 265 nm and using the pre-established calibration curve for 5-FU-COOH (**Fig. S1**). The drug loading through conjugation was four times higher as compared to the passive loading of UCNP@HBP (*i.e.* 12 *vs.* 3 wt%) for the same feed in drug. The drug release of 5-FU-conjugated UCNP@HBP was carried out in PBS (pH 7.4) at 37 °C (**Fig. 2**). The initial burst release was only 12 wt% of 5-FU-COOH within the first 6 h (compared to 68 wt% of 5-FU for passive loading) followed by a sustained release of the drug reaching 64 wt% after 19 days. This initial burst release could be attributed to the presence of free 5-FU-COOH that was not conjugated on the polymer.

2.3. Introduction of redox-degradable branching points on UCNP@HBP

Esterases, often overexpressed in cancer cells, are enzymes able to catalyze the hydrolysis of ester bonds.[43] However, due to the globular structure of the polymer and its constrained conformation due to its grafting on UCNPs along with the large size of esterases, the access of the esterase to the ester groups may be sterically hindered reducing its ability to induce the drug release. Branching points degradable under a stimulus were inserted on UCNP@HBP to break down the polymer providing an easier access of the esterase to the ester linkages between the drug and the polymer. These degradable branching points should be however stable during the circulation of the polymer-drug conjugate in the bloodstream, but able to degrade in cancer cells. Glutathione (GSH) is a tripeptide (L-γ-glutamyl-L-

cysteinyl-glycine) synthesized in the cytosol of mammalian cells and plays an important role in cell function.[44] The intracellular concentration in GSH is higher in most cancer cells as compared to normal cells,[45] *e.g*. 250-2000 and 70-250 nmol per gram of tissue for cancer and disease-free breast tissues respectively, while the extracellular concentration in GSH (2-20 μM) is lower than the intracellular one (2-10 mM).[46] As GSH is able to reduce disulfide bridges, nanohybrids with redox-degradable branching points (UCNP@HBP_{redox}) were prepared similarly using 2-((2-(methacryloyloxy)ethyl)dis-ulfanyl)ethyl 4-cyano-4-(phenylcarbonothioylthio)pentanoate (MA-SS-CPABD) as transmer (**Scheme 2**). TGA of UCNP@HBP_{redox} indicated a content in polymer of 31 wt% (**Fig. S3a**). The amount of MA-SS-CPABD incorporated in the polymer chain of UCNP@HBP_{redox} was determined by UV spectroscopy measuring its depletion in the polymerization medium after removing the nanohybrids as 0.12 mmol per gram of UCNP corresponding to a degree of branching of 0.17. After cleavage of the polymer from the surface of UCNPs by treatment with HF, its number-average molecular weight was determined by size-exclusion chromatography as 363,000 g mol^{-1} (Đ = 9.63) (**Fig. S3b**).

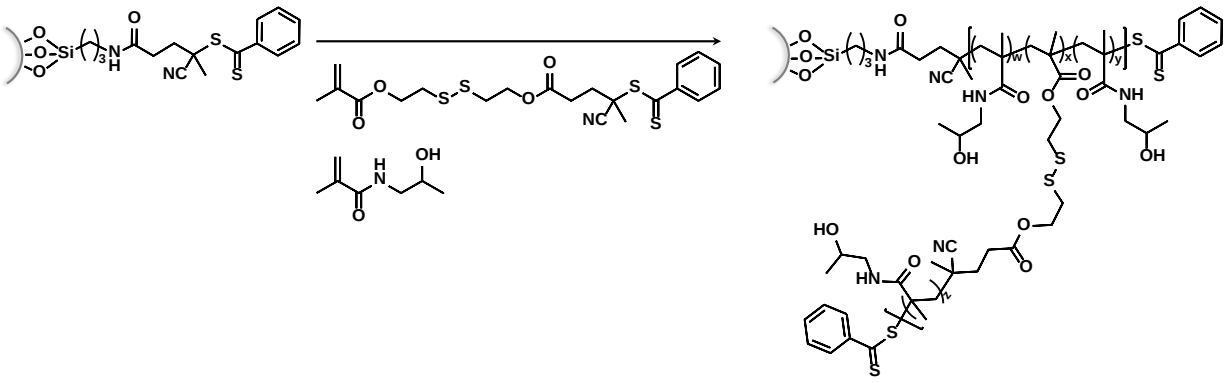

Scheme 2. Synthesis of UCNP@HBP_{redox} by RAFT polymerization from the surface of UCNPs ([UCNP@CPABD] = 10 mg mL^{-1}, [HPMA]:[MA-SS-CPABD]:[AIBN] = 200:1:0.2).

The degradation of the polymer was studied in PBS (pH 7.4) at 37 °C using dithiothreitol (DTT) as reducing agent having a similar activity as glutathione. TGA analysis was used to measure the amount of polymer at the surface of UCNPs for DTT-treated and untreated UCNP@HBP_{redox} exhibiting a weight loss of 5 and 25 wt% respectively (**Fig. 4**). The weight loss of DTT-treated UCNP@HBP_{redox} was similar to UCNP@CPABD suggesting the complete cleavage of the disulfide bridges under these conditions. Dynamic light scattering (DLS) measurement indicated a decrease of the hydrodynamic diameter from 248 to 149 nm upon addition of DTT supporting the degradation of the polymer (**Fig. S4**).

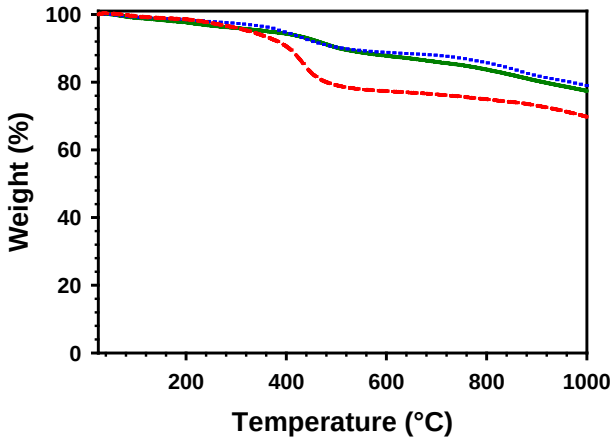

Fig. 4. Degradation of the polymer of UCNP@HBP$_{redox}$ upon addition of 10 mM of DTT in PBS (blue dotted line) by TGA measurement compared to UCNP@CPABD (green solid line) and untreated UCNP@HBP$_{redox}$ (red dashed line).

The polymer of UCNP@HBP$_{redox}$ was labeled with fluorescein isothiocyanate (FITC) by conjugation through the hydroxyl group of the HPMA repeating units. The amount of FITC conjugated was determined by visible spectroscopy at 496 nm using an molar extinction coefficient of 74000 L mol^{-1} cm^{-1} for FITC in water[47] as 1.4 µmol of FITC per gram of FITC-labeled UCNP@HBP$_{redox}$ (**Fig. S5**). The dispersion of UCNP@HBP$_{redox}$ was incubated with DTT to investigate the rate of degradation of the polymer of UCNP@HBP$_{redox}$ by withdrawing aliquots of the supernatant at predetermined time. Under an irradiation at 254 nm, the luminescence of the dispersion of nanohybrids in water (**Fig. S5**) was higher as compared to the control experiment conducted on FITC-labeled UCNP@HBP$_{redox}$ incubated without DTT. The degradation of the polymer upon addition of DTT was quantified by visible spectroscopy at 494 nm of the supernatant (**Fig. 5**). The fraction of fragments of FITC-labeled polymers cleaved from UCNP@HBP$_{redox}$ reached 50% after 30 min of incubation with DTT, which was drastically faster as compared to untreated nanohybrids (4%). The degradation seemed then to decelerate reaching 66% after 120 min (20% for the untreated UCNP@HBP$_{redox}$).

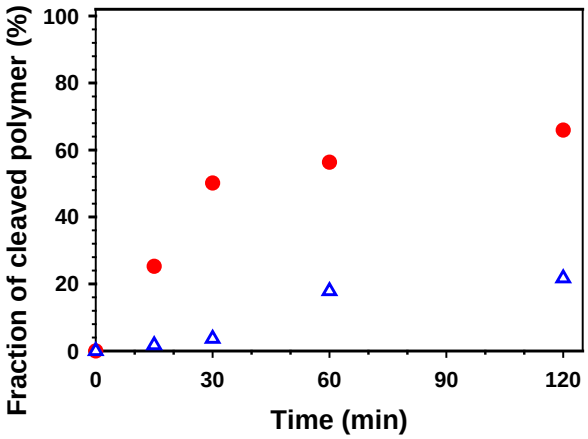

Fig. 5. Rate of degradation of the polymer on FITC-labeled UCNP@HBP$_{redox}$ by monitoring the fraction of polymer cleaved from the nanohybrid with (filled red circles) or without (open blue triangle) incubation in a solution of DTT in PBS (pH 7.4).

3. CONCLUSION

The potential of nanohybrids consisting in UCNPs modified with HPMA-based polymers obtained by RAFT polymerization from the surface of UCNPs for drug vectorization were investigated using 5-FU as model anticancer drug. The introduction of branching points on the polymer led to an increased drug loading in the polymer shell due to the presence of cavities in hyperbranched polymers as compared to linear analogs. As 5-FU loading in UCNP@HBP remained low and was associated to a pronounced burst release of the drug, 5-FU was conjugated to the polymer by esterification reaction. The conjugation induced an increase of 5-FU loading by four folds and more sustained release of the drug. The structure of the polymer was further tuned by introducing redox-degradable branching point using a transmer possessing a disulfide bridge that would be cleaved by glutathione that are present in higher concentration in most cancer cells. The polymer on the nanohybrids was rapidly degraded following their incubation with DTT that should promote the rapid release of the drug once in the cancer cells. As a previous study showed that these UNCPs modified with a polymer shell exhibited a strong emission, these data indicate that these nanohybrids are good candidates for theranostic applications.

4. EXPERIMENTAL

4.1. Materials

1-Hydroxybenzotriazole hydrate (HOBt, ≥97%), 2,2'-azobis(isobutyronitrile) (AIBN, 98%), 4-cyano-4-(thiobenzoylthio)pentanoic acid (CPABD, >98%), dithiothreitol (DTT, ≥98%), phosphate buffered saline tablets (PBS), anhydrous *N*,*N*-dimethylformamide (anhydrous DMF, 99.8%), anhydrous dichloromethane (anhydrous DCM, ≥99.8%), and *N*,*N*-dimethylformamide (DMF, >99%), were purchased from Sigma-

Aldrich. *N*,*N*,*N'*,*N'*-Tetramethyl-O-(1H-benzotriazol-1-yl)uronium hexafluorophosphate (HBTU, 99%) was purchased from Iris Biotech. 2-Hydroxyethyl methacrylate (HEMA, 98%), and 5-fluorouracil (5-FU, 98%) were purchased from ABCR. *N*-Ethyldiisopropylamine (DIPEA, 99%) and 1,4-dioxane (≥99.5%) were purchased from Alfa Aesar. Hydrofluoric acid (HF, 40% in H_2O) was purchased from Ridel de Haen. Methanol (MeOH, 99.8%), ethanol (absolute, 99.99%), cyclohexane (99.8%), acetone (99.8%), and diethyl ether (99%) were purchased from Carlo Erba. Fluorescein 5-isothiocyanate (FITC, 95%) was purchased from TCI. Hydrochloric acid (HCl, 37% in water) was purchased from Fisher Chemical. All chemicals were used as received, except if noted otherwise. AIBN was recrystallized twice from ethanol. $NaYF_4$; Yb 20%; Er 2% upconversion nanoparticles functionalized with 4-cyano-4-(thiobenzoylthio)pentanoic acid (UCNP@CPABD),[26] *N*-(2-hydroxypropyl) methacrylamide (HPMA),[48] 2-(methacryloyloxy)ethyl 4-cyano-4-(phenylcarbonothioylthio)pentanoate (MA-CPABD),[49] 5-fluorouracil-1-acetic acid (5-FU-COOH),[38] and 2-((2-(methacryloyloxy)ethyl)dis-ulfanyl)ethyl 4-cyano-4-(phenylcarbonothioylthio)pentanoate (MA-SS-CPABD)[50] were synthesized as reported in the literature. Dialysis membranes in regenerated cellulose with molecular cutoffs (MWCO) of 1000 and 6000-8000 Da (SpectrumLab) were purchased from Roth.

4.2. Characterization

UV-vis spectroscopy was carried out using a Perkin Elmer Lambda 25 spectrophotometer into quartz cuvettes at room temperature. Dynamic light scattering (DLS) experiments were performed in triplicate on a Malvern Zetasizer Nano ZS at 633 nm (He-Ne laser beam) with a scattering angle fixed at 173° at 25 °C. Before measurement, the solutions were filtered through a 0.45 µm syringe filter. Fourier transform infrared (FTIR) spectra were recorded on a Bruker Vertex 70 spectrometer using the attenuated total reflectance (ATR) technique for wavenumber between 600 and 4000 cm^{-1}. ^1H and ^{13}C NMR spectra were recorded in MeOD on a 400 MHz Bruker Avance III HD spectrometers equipped with a BBO type probe at 25 °C. Size-exclusion chromatography (SEC) was performed on DIONEX Ultimate 3000 system equipped with a guard column and four Shodex OH-pak columns (7.5 x 300 mm, 803HQ, 804HQ, 806HQ, 807HQ), a Wyatt OPTILAB rEX differential refractometer, and a Wyatt DAWN HELEOS II light scattering detector and was operated at 30 °C using 60/40 water/acetonitrile with 0.1 M $NaNO_3$ as eluent at a flow rate of 0.5 mL min^{-1}. Mass measurements were carried out on a Bruker Daltonics microTOF spectrometer (Bruker Daltonik GmgH, Bremen, Germany) equipped with an orthogonal electrospray (ESI) interface. Calibration was performed using Tunning mix (Agilent Technologies). Sample solutions were introduced into the spectrometer source with a syringe pump (Harvard type 55 1111: Harvard Apparatus Inc., South Natick, MA, USA) with a flow rate of 5 µL min^{-1}. Thermogravimetric analyses (TGA) were performed on a

Mettler-Toledo TGA2 thermogravimeter. The measurements were conducted from 25 to 1000 °C at a heating scan rate of 50 °C min^{-1} using alumina crucibles under a N_2 atmosphere (gas flow rate: 100 mL min^{-1}).

4.3. RAFT polymerization from UCNP@CPABD. All the polymerizations were conducted using UCNP@CPABD having 3.1 CPABD per square nanometer of UCNPs. Briefly, 30 mg of UCNP@CPABD (7.2 μmol of CPABD on nanohybrids), 250 mg of HPMA (1.7 mmol), and 3 mL of 1,4-dioxane were placed in a 5 mL round-bottom flask. For the synthesis of UCNP@polyHPMA 2.5 mg of CPABD (9 μmol) was added, while 9 μmol of transmer (3.5 mg of MA-CPABD or 4.4 mg of MA-SS-CPABD for the synthesis of UCNP@HBP or UCNP@HBP_{redox} respectively) were used. The polymerization mixture was sonicated for 6 min twice in a water bath with some ice (approximatively 15 °C) and then 0.3 mg of AIBN (2 μmol) dissolved in 50 μL of 1,4-dioxane was added. The polymerization medium was degassed by bubbling argon in the solution for 30 min before stirring it in an oil bath thermostated at 65 °C for 24 h. After cooling the flask in an ice-water bath, the nanohybrids were isolated by centrifugation and purified by performing cycles of redispersion and centrifugation successively in 1,4-dioxane, MeOH and acetone (three times for each solvent). For SEC measurement, the polymer was cleaved from the UCNPs by dispersing 30 mg of the nanohybrids in 2.5 mL of deionized water then 0.5 mL of 40 % HF was added (Caution: HF is highly corrosive). The solution was then stirred for 4 h, neutralized by adding slowly a saturated solution of $NaHCO_3$, dialyzed against water (dialysis membrane with a MWCO of 1000 Da), and centrifuged to collect the supernatant that was lyophilized.

4.4. Passive loading of 5-FU in UCNP@polyHPMA and UCNP@HBP

1 to 5 mg of 5-FU was dissolved in 0.5 mL of water, while 5 mg of nanohybrids were dispersed in 1 mL of water. These solutions were sonicated for 30 s, combined, sonicated again for 30 s, and shacked on an orbital shaker at room temperature for 24 h. The dispersion was centrifuged at 6,500 g at room temperature for 10 min. The supernatant was discarded and the loaded nanohybrids were washed by redispersion in 1 mL of water using a vortex mixer, centrifugation, and recovery of the nanohybrids before drying them under vacuum. The quantification of the amount of 5-FU loaded in the nanohybrids was performed by dispersing 2.5 mg of loaded nanohybrids in 2 mL of reverse osmosis (RO) water that was shaken for 48 h. To avoid the saturation of the solution, the supernatant was collected after centrifugation and the UCNPs were redispersed in fresh distilled water after 3, 6, and 24 h. The supernatants were combined and the volume was adjusted to 25 mL. The absorbance value of 5-FU was determined at 265 nm by UV spectroscopy and used to determine the amount of drug from a pre-established calibration

curve of 5-FU in RO water permitting the calculation of the drug loading ([$m_{drug\ in\ nanohybrid}/m_{nanohydrid}$] x 100) and encapsulation efficiency ([$m_{drug\ in\ nanohybrid}/m_{drug\ in\ feed}$] x 100).

4.5. Conjugation of 5-FU on UCNP@HBP

10 mg of UCNP@HBP dispersed in 2 mL of anhydrous DMF were sonicated for 1 min twice. 10 mg of 5-FU-COOH (54 μmol) and 41 mg of HBTU (108 μmol) were dissolved in 1 mL of anhydrous DMF that were placed in an ice bath for 10 min before adding 0.04 mL of DIPEA (216 μmol). After 10 min, the dispersion of UCNP@HBP was added dropwise and the mixture was allowed to stir overnight at room temperature. The solution was centrifuged and the particles were collected. Cycles of centrifugation and redispersion in DMF and water were repeated at least five times to ensure that no free drug remained at the surface of the nanohybrids before lyophilizing them. To determine the amount of 5-FU conjugated on the nanohybrids, the drug was cleaved using KOH and quantified by UV spectroscopy. Briefly, 2 mg of 5-FU-conjugated UCNP@HBP were dispersed in 2 mL of 50/50 water/THF and sonicated for 1 min. 95 mg of KOH were added to the solution and stirred overnight in an oil bath thermostated at 50 °C. The mixture was centrifuged and the supernatant was collected. Cycles of centrifugation and redispersion in water were repeated three times. The supernatants were combined, concentrated by rotary evaporation, neutralized with diluted HCl, and placed in a 25 mL volumetric flask that was filled with RO water. This solution was used for characterization by UV-vis spectroscopy at 275 nm to determine the concentration in drug using a pre-established calibration curve. Drug loading and encapsulation efficiency were calculated as previously.

4.6. 5-FU release study

Drug release studies were carried out in PBS buffer (pH 7.4) at 37 °C. Briefly, 2 mg of nanohybrids were dispersed into 2 mL of PBS buffer. The solution was dialyzed (dialysis membrane with a MWCO of 6000-8000 Da) against 50 mL of PBS buffer at 37 °C under gentle agitation. 2 mL of the release medium was withdrawn at predetermined times and replaced with an equal volume of fresh medium to keep the total volume constant. The concentration in 5-FU was determined by measuring its absorbance at 265 nm by UV spectroscopy permitting to calculate the drug release percentage with respect to the initial drug content ([m_t/m_0] x 100, where m_0 and m_t represent the weight of loaded and released drug at time t, respectively).

4.7. Polymer degradation study of UCNP@HBP$_{redox}$ in the presence of DTT

20 mg of UCNP@HBP$_{redox}$ were dispersed in 4 mL of PBS (pH = 7.4) by sonication and the solution was divided into two parts. The first part was used to evaluate the redox degradation of the polymer through addition of 2 mL of 20 mM of DTT in PBS, while the second one was a control and 2 mL of PBS (pH = 7.4)

was added. The solutions were shaken at 37 °C for 24 h. The nanoparticles were isolated by centrifugation and washed several times with distilled water. 10 mg of nanoparticles were dispersed in 1 mL of RO water by sonication. One drop of this dispersion was diluted into 1.5 mL of RO water, filtered (0.45 µm, nylon certified HPLC), and used for DLS measurement. The nanoparticles were isolated by centrifugation, dried under vacuum for 48 h and used for TGA measurement to determine the remaining amount of polymer grafted on UCNPs.

4.8. Conjugation of FITC on UCNP@HBP$_{redox}$

30 mg of UCNP@HBP dispersed in 4 mL of anhydrous DMF were sonicated for 1 min twice. 10 mg of FITC (0.026 mmol) was added under argon and the reaction mixture was stirred at room temperature in the dark for 24 h. The dispersion was centrifuged to collect the nanohybrids. Cycles of centrifugation and redispersion first in DMF and then in water were done at least five times for each solvent to ensure the full removal of unreacted FITC. The nanohybrids were freeze-dried affording 27 mg of a light-yellow powder. The concentration in FITC on UCNP@HBP$_{redox}$ was determined by measuring its absorbance at 496 nm by visible spectroscopy using a molar extinction coefficient of 74000 L mol^{-1} cm^{-1}.[47] The degradation rate of the polymer in the presence of DTT was performed as previously withdrawing the supernatant after centrifugation and redispersing the nanohybrids in fresh DTT solution at 15, 30, 60, 120, and 360 min and measuring the absorbance at 496 nm.

CREDIT AUTHORSHIP CONTRIBUTION STATEMENT

Alireza Kavand: conceptualization, methodology, investigation, visualization, writing; **Nicolas Anton:** supervision; **Thierry Vandamme:** supervision; **Christophe Serra:** funding acquisition, supervision; **Delphine Chan-Seng:** funding acquisition, conceptualization, supervision, visualization, writing.

DATA AVAILABILITY

The raw/processed data required to reproduce these findings cannot be shared at this time due to technical or time limitations.

APPENDIX A. Supplementary material

Supplementary data to this article can be found online at .

ACKNOWLEDGMENTS

This work was funded by the French National Research Agency (ANR) through the Programme d'Investissement d'Avenir under contract ANR-11-LABX-0058_NIE within the Investissement d'Avenir program ANR-10-IDEX-0002-02. This work was financially supported by the CNRS and the University of Strasbourg. The doctoral position of AK is supported by the University of Strasbourg through a doctoral contract from the Physics and Chemistry-Physics doctoral school and his postdoctoral position by the Investissement d'Avenir program. The authors thank the polymer characterization facilities at the Institut Charles Sadron, the electron microscopy facilities at the Institut Charles Sadron, the mass spectrometry facilities of the University of Strasbourg, and the Cronenbourg NMR core facilities.

REFERENCES

[1] S.S. Kelkar, T.M. Reineke, Theranostics: Combining imaging and therapy, Bioconjugate Chem. 22 (2011) 1879-1903.

[2] J.O. Escobedo, O. Rusin, S. Lim, R.M. Strongin, NIR dyes for bioimaging applications, Curr. Opin. Chem. Biol. 14 (2010) 64-70.

[3] P. Sharma, S. Brown, G. Walter, S. Santra, B. Moudgil, Nanoparticles for bioimaging, Adv. Colloid Interface Sci. 123-126 (2006) 471-485.

[4] Z. Shen, A. Wu, X. Chen, Iron oxide nanoparticle based contrast agents for magnetic resonance imaging, Mol. Pharmaceutics 14 (2017) 1352-1364.

[5] Y. Bao, J.A. Sherwood, Z. Sun, Magnetic iron oxide nanoparticles as T_1 contrast agents for magnetic resonance imaging, J. Mater. Chem. C 6 (2018) 1280-1290.

[6] I.V. Martynenko, A.P. Litvin, F. Purcell-Milton, A.V. Baranov, A.V. Fedorov, Y.K. Gun'ko, Application of semiconductor quantum dots in bioimaging and biosensing, J. Mater. Chem. B 5 (2017) 6701-6727.

[7] S. Pandey, D. Bodas, High-quality quantum dots for multiplexed bioimaging: A critical review, Adv. Colloid Interface Sci. 278 (2020) 102137.

[8] X. Wu, G. Chen, J. Shen, Z. Li, Y. Zhang, G. Han, Upconversion nanoparticles: A versatile solution to multiscale biological imaging, Bioconjugate Chem. 26 (2015) 166-175.

[9] G. Chen, H. Qiu, P.N. Prasad, X. Chen, Upconversion nanoparticles: Design, nanochemistry, and applications in theranostics, Chem. Rev. 114 (2014) 5161-5214.

[10] J. Zhou, Q. Liu, W. Feng, Y. Sun, F. Li, Upconversion luminescent materials: Advances and applications, Chem. Rev. 115 (2015) 395-465.

[11] J. Jin, Y.-J. Gu, C.W.-Y. Man, J. Cheng, Z. Xu, Y. Zhang, H. Wang, V.H.-Y. Lee, S.H. Cheng, W.-T. Wong, Polymer-coated $NaYF_4$:Yb^{3+}, Er^{3+} upconversion nanoparticles for charge-dependent cellular imaging, ACS Nano 5 (2011) 7838-7847.

[12] H.T.T. Duong, Y. Chen, S.A. Tawfik, S. Wen, M. Parviz, O. Shimoni, D. Jin, Systematic investigation of functional ligands for colloidal stable upconversion nanoparticles, RSC Adv. 8 (2018) 4842-4849.

[13] P. Li, L. Liu, J. Zhou, L. Zhao, H. Fan, X. Huang, Thermo-activatable PNIPAM-functionalized lanthanide-doped upconversion luminescence nanocomposites used for in vitro imaging, RSC Adv. 7 (2017) 50643-50647.

[14] I. Recalde, N. Estebanez, L. Francés-Soriano, M. Liras, M. González-Béjar, J. Pérez-Prieto, Upconversion nanoparticles with a strong acid-resistant capping, Nanoscale 8 (2016) 7588-7594.

[15] J.-C. Boyer, M.-P. Manseau, J.I. Murray, F.C.J.M. van Veggel, Surface modification of upconverting $NaYF_4$ nanoparticles with PEG−phosphate ligands for NIR (800 nm) biolabeling within the biological window, Langmuir 26 (2010) 1157-1164.

[16] Y. Que, C. Feng, G. Lu, X. Huang, Polymer-coated ultrastable and biofunctionalizable lanthanide nanoparticles, ACS Appl. Mater. Interfaces 9 (2017) 14647-14655.

[17] W. Wu, L. Wang, J. Yuan, Z. Zhang, X. Zhang, S. Dong, J. Hao, Formation and degradation tracking of a composite hydrogel based on UCNPs@PDA, Macromolecules 53 (2020) 2430-2440.

[18] Q. Xiao, Y. Ji, Z. Xiao, Y. Zhang, H. Lin, Q. Wang, Novel multifunctional $NaYF_4$:Er^{3+},Yb^{3+}/PEGDA hybrid microspheres: NIR-light-activated photopolymerization and drug delivery, Chem. Commun. 49 (2013) 1527-1529.

[19] S. Beyazit, S. Ambrosini, N. Marchyk, E. Palo, V. Kale, T. Soukka, B. Tse Sum Bui, K. Haupt, Versatile synthetic strategy for coating upconverting nanoparticles with polymer shells through localized photopolymerization by using the particles as internal light sources, Angew. Chem. Int. Ed. 53 (2014) 8919-8923.

[20] L. Zhou, B. He, J. Huang, Z. Cheng, X. Xu, C. Wei, Multihydroxy dendritic upconversion nanoparticles with enhanced water dispersibility and surface functionality for bioimaging, ACS Appl. Mater. Interfaces 6 (2014) 7719-7727.

[21] B. He, L. Zhou, Efficient tailoring of the surface of upconversion nanoparticles via surface-initiated cationic ring-opening polymerization, RSC Adv. 5 (2015) 97764-97772.

[22] Z. Li, X. Zou, F. Shi, R. Liu, Y. Yagci, Highly efficient dandelion-like near-infrared light photoinitiator for free radical and thiol-ene photopolymerizations, Nat. Commun. 10 (2019) 3560.

[23] J. Xiang, X. Tong, F. Shi, Q. Yan, B. Yu, Y. Zhao, Near-infrared light-triggered drug release from UV-responsive diblock copolymer-coated upconversion nanoparticles with high monodispersity, J. Mater. Chem. B 6 (2018) 3531-3540.

[24] A. Bagheri, H. Arandiyan, N.N.M. Adnan, C. Boyer, M. Lim, Controlled direct growth of polymer shell on upconversion nanoparticle surface via visible light regulated polymerization, Macromolecules 50 (2017) 7137-7147.

[25] Z. Xie, X. Deng, B. Liu, S. Huang, P. Ma, Z. Hou, Z. Cheng, J. Lin, S. Luan, Construction of hierarchical polymer brushes on upconversion nanoparticles via NIR-light-initiated RAFT polymerization, ACS Appl. Mater. Interfaces 9 (2017) 30414-30425.

[26] A. Kavand, C. Blanck, F. Przybilla, Y. Mély, N. Anton, T. Vandamme, C.A. Serra, D. Chan-Seng, Investigating the growth of hyperbranched polymers by self-condensing vinyl RAFT copolymerization from the surface of upconversion nanoparticles, Polym. Chem. 11 (2020) 4313-4325.

[27] J. Arias, Novel strategies to improve the anticancer action of 5-fluorouracil by using drug delivery systems, Molecules 13 (2008) 2340-2369.

[28] D.B. Longley, D.P. Harkin, P.G. Johnston, 5-Fluorouracil: Mechanisms of action and clinical strategies, Nat. Rev. Cancer 3 (2003) 330-338.

[29] G.A. Caballero, R.K. Ausman, E.J. Quebbeman, Long-term, ambulatory, continuous IV infusion of 5-FU for the treatment of advanced adenocarcinomas, Cancer Treat. Rep. 69 (1985) 13-15.

[30] A. Shah, W. MacDonald, J. Goldie, G. Gudauskas, B. Brisebois, 5-FU infusion in advanced colorectal cancer: A comparison of three dose schedules, Cancer Treat. Rep. 69 (1985) 739-742.

[31] B. Arıca, S. Çalış, H.S. Kaş, M.F. Sargon, A.A. Hıncal, 5-Fluorouracil encapsulated alginate beads for the treatment of breast cancer, Int. J. Pharm. 242 (2002) 267-269.

[32] M. Boisdron-Celle, P. Menei, J.P. Benoit, Preparation and characterization of 5-fluorouracil-loaded microparticles as biodegradable anticancer drug carriers, J. Pharm. Pharmacol. 47 (1995) 108-114.

[33] J.L. Arias, M.A. Ruiz, M. López-Viota, Á.V. Delgado, Poly(alkylcyanoacrylate) colloidal particles as vehicles for antitumour drug delivery: A comparative study, Colloids Surf. B 62 (2008) 64-70.

[34] B. Elorza, M.A. Elorza, G. Frutos, J.R. Chantres, Characterization of 5-fluorouracil loaded liposomes prepared by reverse-phase evaporation or freezing-thawing extrusion methods: Study of drug release, Biochim. Biophys. Acta Biomembr. 1153 (1993) 135-142.

[35] M. Malet-Martino, R. Martino, Clinical studies of three oral prodrugs of 5-fluorouracil (Capecitabine, UFT, S-1): A review, Oncologist 7 (2002) 288-323.

[36] Z. Dong, W. Zheng, Z. Xu, Z. Yin, Improved stability and tumor targeting of 5-fluorouracil by conjugation with hyaluronan, J. Appl. Polym. Sci. 130 (2013) 927-932.
[37] G.-P. Yan, R.-X. Zhuo, C.-Y. Zheng, Study on the anticancer drug 5-fluorouracil-conjugated polyaspartamide containing hepatocyte-targeting group, J. Bioact. Compat. Polym. 16 (2001) 277-293.
[38] Z.-J. Sun, B. Sun, C.-W. Sun, L.-B. Wang, X. Xie, W.-C. Ma, X.-L. Lu, D.-L. Dong, A poly(glycerol-sebacate-(5-fluorouracil-1-acetic acid)) polymer with potential use for cancer therapy, J. Bioact. Compat. Polym. 27 (2012) 18-30.
[39] M. Islami, A. Zarrabi, S. Tada, M. Kawamoto, T. Isoshima, Y. Ito, Controlled quercetin release from high-capacity-loading hyperbranched polyglycerol-functionalized graphene oxide, Int. J. Nanomed. 13 (2018) 6059-6071.
[40] O. Perumal, J. Khandare, P. Kolhe, S. Kannan, M. Lieh-Lai, R.M. Kannan, Effects of branching architecture and linker on the activity of hyperbranched polymer-drug conjugates, Bioconjugate Chem. 20 (2009) 842-846.
[41] R. Duncan, Development of HPMA copolymer–anticancer conjugates: Clinical experience and lessons learnt, Adv. Drug Deliv. Rev. 61 (2009) 1131-1148.
[42] P.T. Wong, S.K. Choi, Mechanisms of drug release in nanotherapeutic delivery systems, Chem. Rev. 115 (2015) 3388-3432.
[43] C.A. McGoldrick, Y.-L. Jiang, V. Paromov, M. Brannon, K. Krishnan, W.L. Stone, Identification of oxidized protein hydrolase as a potential prodrug target in prostate cancer, BMC Cancer 14 (2014) 77.
[44] K. Aquilano, S. Baldelli, M.R. Ciriolo, Glutathione: New roles in redox signaling for an old antioxidant, Front. Pharmacol. 5 (2014) 196.
[45] M.P. Gamcsik, M.S. Kasibhatla, S.D. Teeter, O.M. Colvin, Glutathione levels in human tumors, Biomarkers 17 (2012) 671-691.
[46] H. Sun, F. Meng, R. Cheng, C. Deng, Z. Zhong, Reduction-sensitive degradable micellar nanoparticles as smart and intuitive delivery systems for cancer chemotherapy, Expert Opin. Drug Delivery 10 (2013) 1109-1122.
[47] W. Wang, Y. Zhang, Y. Liu, Y. He, Highly selective and sensitive ratiometric fluorescent polymer dots for detecting hypochlorite in 100% aqueous media, Spectrochim. Acta Part A 207 (2019) 73-78.
[48] K. Ulbrich, V. Šubr, J. Strohalm, D. Plocová, M. Jelínková, B. Říhová, Polymeric drugs based on conjugates of synthetic and natural macromolecules: I. Synthesis and physico-chemical characterisation, J. Controlled Release 64 (2000) 63-79.

[49] Z. Wei, X. Hao, P.A. Kambouris, Z. Gan, T.C. Hughes, One-pot synthesis of hyperbranched polymers using small molecule and macro RAFT inimers, Polymer 53 (2012) 1429-1436.
[50] L. Tao, J. Liu, B.H. Tan, T.P. Davis, RAFT synthesis and DNA binding of biodegradable, hyperbranched poly(2-(dimethylamino)ethyl methacrylate), Macromolecules 42 (2009) 4960-4962.